In-Place Strength of Welded Headed Studs

A. Fattah Shaikh
Professor
Department of Civil Engineering
University of Wisconsin — Milwaukee
Milwaukee, Wisconsin

Whayong Yi
Structural Engineer
Graef, Anhalt, Schloemer
and Associates
Milwaukee, Wisconsin

In designing welded headed studs, it is common practice to calculate strengths based on concrete failure and steel failure separately, and use the lesser of the two as the in-place strength.

It is generally agreed that there are only minor differences between the various design procedures for determining the strength of welded headed studs based on steel failure. However, there are concerns that serious discrepancies occur in the different design methods used to calculate the strength based on concrete failure. These concerns stemmed from a comparative analysis of tension strength conducted by Klingner and Mendonca.[1]

To resolve these conflicts, a task group under the auspices of the PCI Connection Details Committee studied the problem of tension strength based on concrete failure. As a result of this study, the Connections Committee has proposed a revision of the tension strength equation in the *PCI Design Handbook*.[2] The proposed revision, its justification and its impact on other aspects, such as group action, behavior under combined loads, and also an analysis of the direct shear strength, are given in this paper.

Various analyses in this article focus on strengths as governed by the concrete failure; however, for the sake of completeness, the proposed design procedure includes an analysis of steel failure. The equations for steel failure are taken from the *PCI Design Handbook*.[2] As noted previously, these equations generally agree with other recommendations and, therefore, no revision is considered necessary at this time.

The design procedure described herein is proposed as a replacement for the corresponding material in the *PCI Design Handbook*[2] and also for inclusion in the *PCI Connection Manual*[3] currently under revision. Although the paper focuses on welded headed studs, the design equations would also apply to nut/washer anchor bolts[4,5] and other similar inserts, such as loop inserts,[3,6,7] and expansion anchors.[8]

Synopsis

Based on a review of the state-of-the-art, the authors present a design procedure for welded headed studs and propose its adoption in the revised editions of the *PCI Design Handbook* and the *PCI Connection Details Manual*.

Numerical examples are included to illustrate the application of the proposed method.

TENSION STRENGTH

The tension strength of a typical connection may be limited by the sum of strengths of individual studs in the connection. Therefore, the tension strength of an isolated stud is discussed first and then is followed with discussions of member edge proximity and distance between studs.

Tension Strength of an Isolated Stud (No Edge Effect)

The failure in concrete due to tension load on a stud is known to occur along a conical surface as shown in Fig. 1. The angle of the cone (angle α) varies, but for design purposes, a value of 45 deg has been typically used to define the failure surface.

The tension (pull-out strength) associated with this failure is based on either the actual cone surface area times an average uniform stress[2,3,5,8,10] or a pseudo area times an average uniform stress. Two commonly used models for determining the pseudo area are shown in Fig. 1: (1) the projected circle[11,12] with surface area A_{pc}, and (2) the concentric cylinder[6,7] with surface area A_{cy}.

There is a small difference in the definition of projected circle between Refs. 11 and 12. The TVA Standard[11] uses the full circle while ACI 349[12] reduces the projected circle by the smaller circle corresponding to the stud head. In most cases, the two definitions will yield close results; however, the definition of ACI 349[12] appears more rational since it takes appropriate account of the discontinuity (stud head intrusion) in concrete and, therefore, it is used here.

The relationship between various surface areas is dependent upon the angle α and is shown in Fig. 1 for two different embedment lengths. For α = 45 deg, the various surface areas are:

Cone surface:

$$A_n = \sqrt{2}\,\pi l_e (l_e + d_h) \qquad (1)$$

Projected circle (Ref. 12):

$$A_{pc} = \pi l_e (l_e + d_h) \qquad (2)$$

Concentric cylinder (Ref. 7):

$$A_{cy} = \pi l_e (l_e + d_h) \qquad (3)$$

Note that while the projected circle and concentric cylinder have equal areas, the cone surface area is $\sqrt{2}$ times as much. However, this observation is only true for angle α = 45 deg (Fig. 1).

The tension strength using these areas is obtained by multiplying the area with an average uniform stress. Interestingly, the same level of average uniform stress, namely $4\sqrt{f'_c}$, has been used with different areas presumably based on differing levels of correlation (lower bound versus median). This assumption results in the carry over of the $\sqrt{2}$ factor from the area relationship to the tension strength relationship. The resulting tension strength* equations are:

*In the body of this paper, reference is generally made to nominal strength. The strength reduction factor (ϕ) is incorporated in the design procedure.

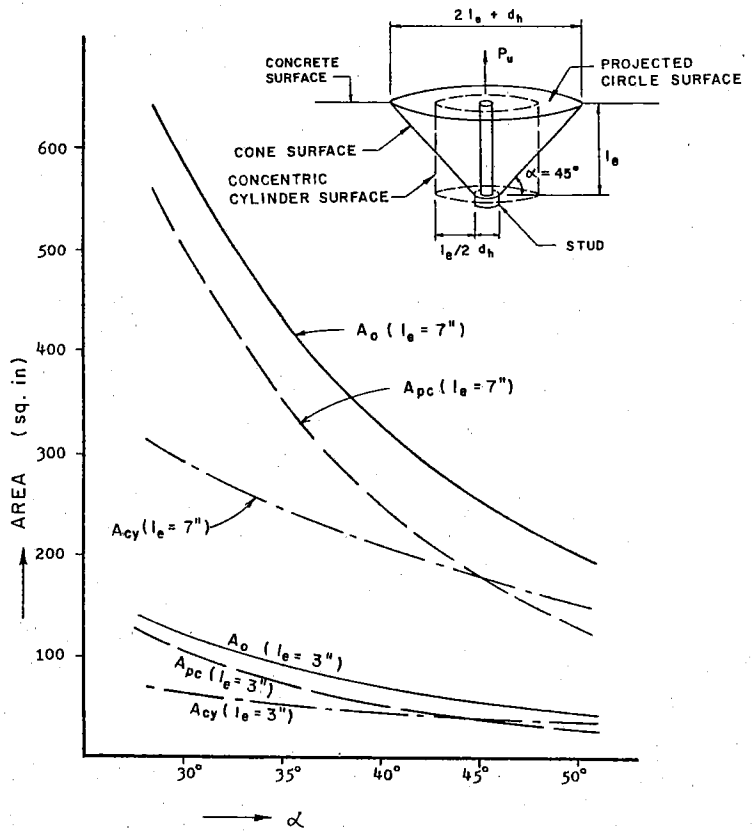

Fig. 1. Failure surfaces for stud under tension load.

Using the cone surface:

$$P_{nc} = 4\ \sqrt{f'_c} A_o = 4\ \sqrt{f'_c}\ [\sqrt{2}\,\pi\, l_e\,(l_e + d_h)] \quad (4)$$

Using the projected circle or concentric cylinder:

$$P_{nc} = 4\ \sqrt{f'_c}\, A_{pc}\ (\text{or}\, A_{cy})$$
$$= 4\ \sqrt{f'_c}\ [\pi(l_e + d_h)] \quad (5)$$

Correlation With Test Data

Klingner and Mendonca[1] have reported a compilation of available test data and correlations with different design equations. The portion of this data where concrete failure is indicated is plotted in Figs. 2 through 6 in a different form to get a better appreciation for the edge effect as discussed in the next section.

There are 38 data points, of which 25 include the edge effect and 13 do not. Two of the data points pertain to lightweight concrete, the remaining 36 to normal weight concrete. Also indicated in Figs. 2 through 6 is a simple count related to conservative/nonconservative correlation with respect to the $\phi = 1.0$ line.

Given the limited number of data points coupled with large scatter, it

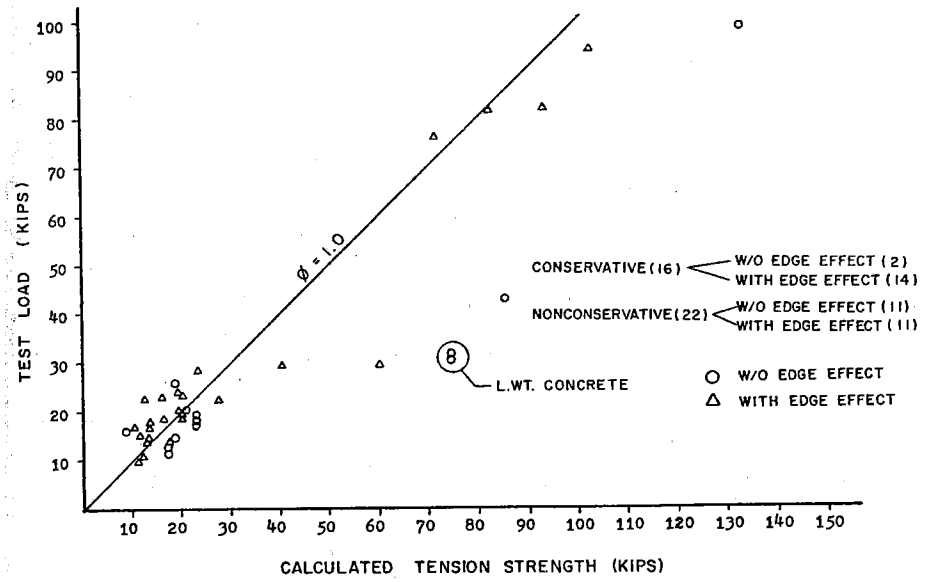

Fig. 2. Calculated tension strength (Refs. 2 and 9) versus test load.

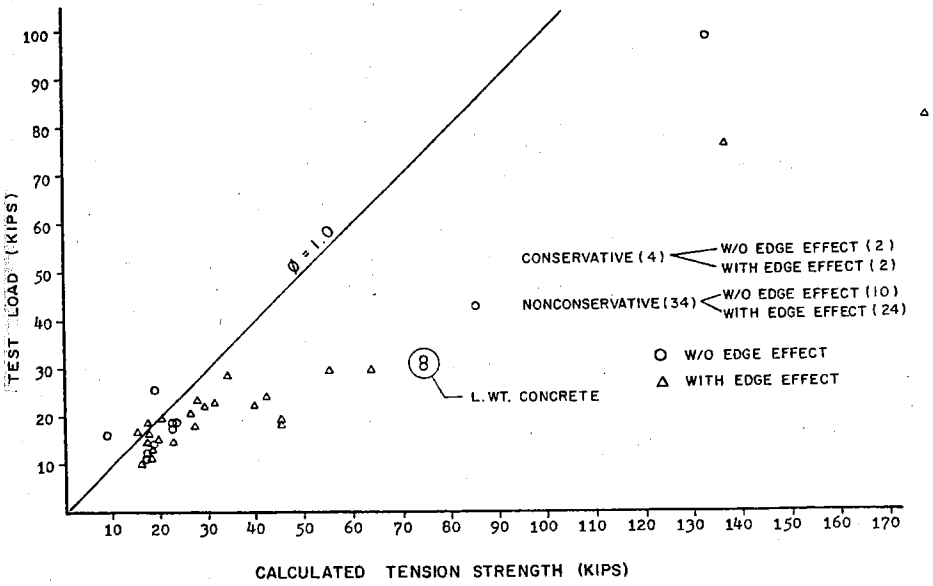

Fig. 3. Calculated tension strength (PCI Manual for Structural Design of Architectural Precast Concrete[5]) versus test load.

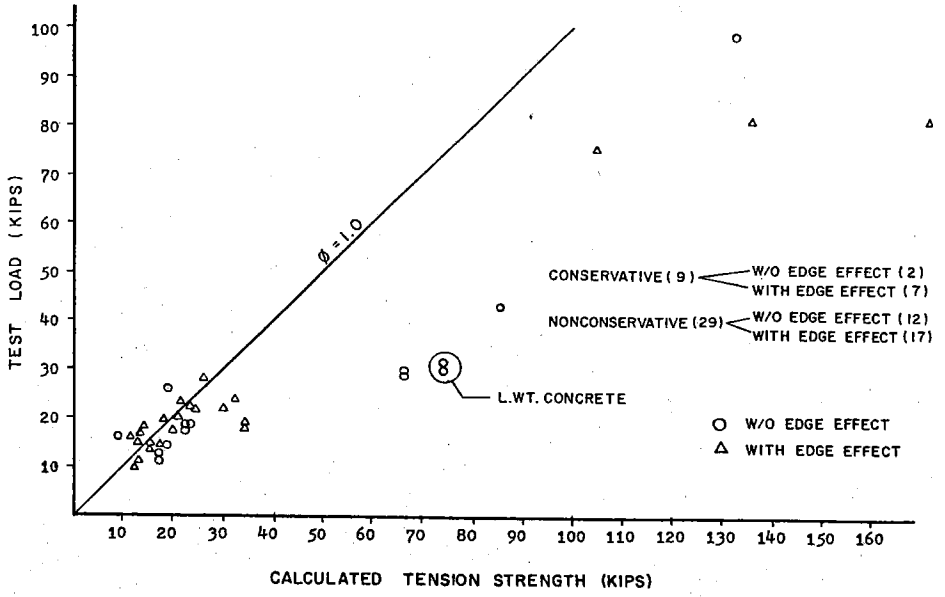

Fig. 4. Calculated tension strength (TRW-Nelson Design Data 10[10]) versus test load.

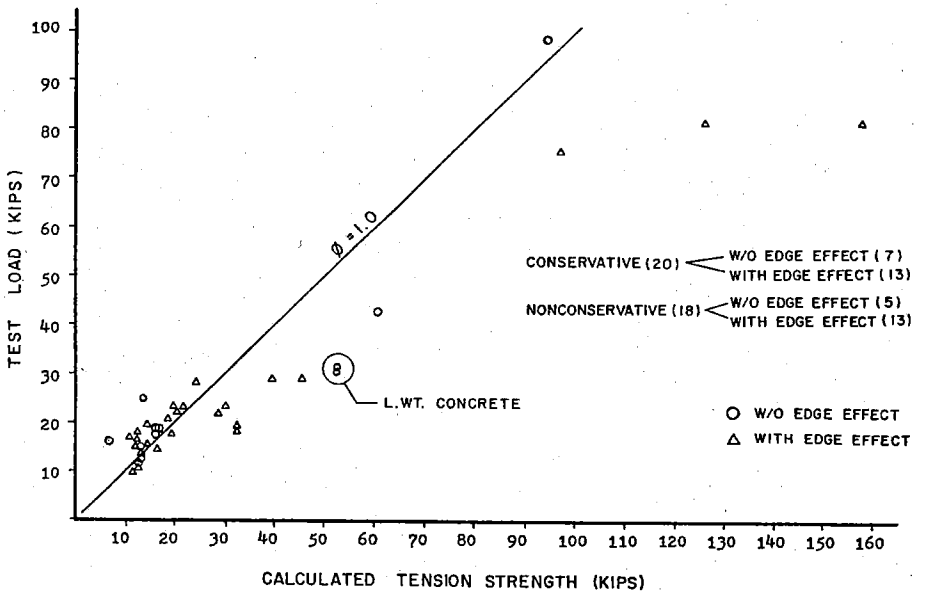

Fig. 5. Calculated tension strength (TVA Civil Design Standard[11]) versus test load.

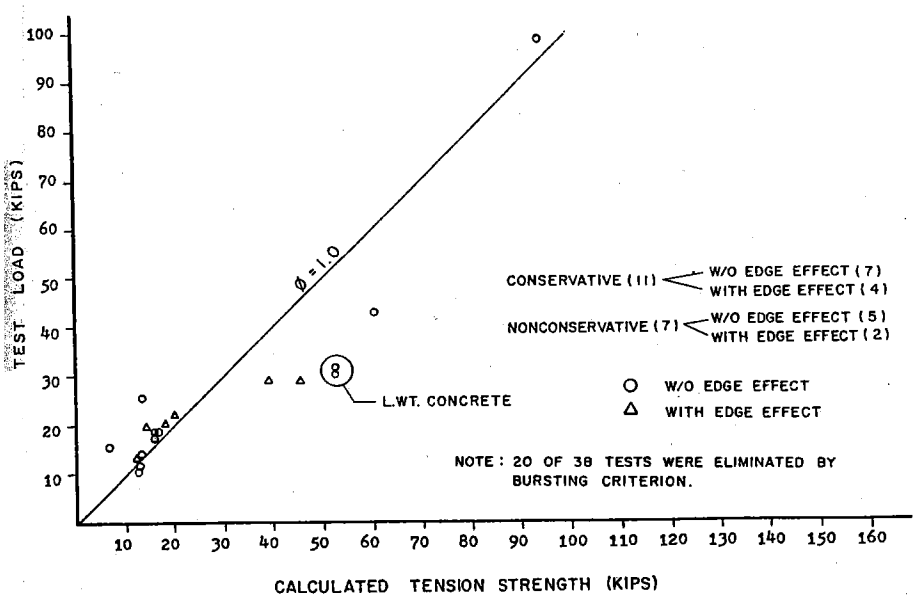

Fig. 6. Calculated tension strength (ACI 349[12]) versus test load.

seems reasonable to base the nominal strength equations on the lower bound correlations — an observation with which there appears to be a general consensus within the Connection Details Committee. As shown in Figs. 2 through 6, except for perhaps the ACI 349 procedure[12] (Fig. 6), all other approaches do not correspond to a lower bound. Specifically, the concern expressed regarding the strength equations in the *PCI Design Handbook*[2] (Fig. 2) is valid. This concern has led many members of the Connection Details Committee and others to suggest dropping $\sqrt{2}$ from Eq. (4).

Acceptance of this suggestion may be interpreted as lowering of the average uniform stress in Eq. (4) from a value of $4\sqrt{f'_c}$ to $(4/\sqrt{2})\sqrt{f'_c}$ and thus Eq. (4) may be written as:

$$P_{nc} = \frac{4}{\sqrt{2}}\sqrt{f'_c}A_o$$

$$P_{nc} = \frac{4}{\sqrt{2}}\sqrt{f'_c}[\sqrt{2}\pi l_e(l_e + d_h)] \quad (6)$$

Eqs. (5) and (6) will now produce identical correlations and the actual correlation with data points without the edge effect is shown in Fig. 7. Ignoring the two lightweight concrete data points and the one stray data point for normal weight concrete, the correlation is good. Therefore, any of three models, i.e., the cone, the projected circle or the concentric cylinder, may be used for calculating the nominal tension strength of an isolated stud.

The projected circle model is simple and its adoption would result in consistency with ACI 349.[12] The analogy of the concentric cylinder with punching shear in footings and slabs is appealing. However, both these models deal with the question in a pseudo manner. The cone model relates to actual failure surface and affords the flexibility of potential

future refinements with respect to angle α. The Connection Details Committee has recommended use of the cone model [Eq. (6)] with the constant $4/\sqrt{2}$ rounded off to 2.8.

With respect to lightweight concrete, there are only two data points available and thus a meaningful analysis is not feasible. Until more data is available, use of the usual factor λ (equal to 1.0 for normal weight concrete, 0.85 for sand lightweight concrete, and 0.75 for all lightweight concrete) has been retained by the Connection Details Committee.

Thus, the equation included in the design procedure is:

$$P_{nc} = 2.8\,\lambda\sqrt{f'_c}A_o \qquad (7)$$

Consideration of Edge Effect

Vicinity of inserts to concrete edges appears to affect the pull-out strength in two ways: (1) direct reduction of surface area and (2) reduction in the available tension strength of concrete. Whereas the first effect is obvious and easily taken care of by using the reduced area of the failure surface, the second effect has not been directly recognized in the pull-out strength equations.

This second effect is analogous to the transition of shear stress from $4\sqrt{f'_c}$ to $2\sqrt{f'_c}$ as the mode of shear failure in footings/slabs changes from a punching condition to a one-way condition (ACI 318-83[13]). Recognition of this effect also is reflected in the *PCI Design Handbook*[2] for the design of beam ledges.

Ref. 5 takes account of the edge effect by simply multiplying the full cone based pull-out strength by the ratio of partial cone area to full cone area. Refs. 11 and 12 use the projected partial circle to full circle area ratio.

These approaches, however, take only one of the two parts of edge effect into account and are likely to result in poor

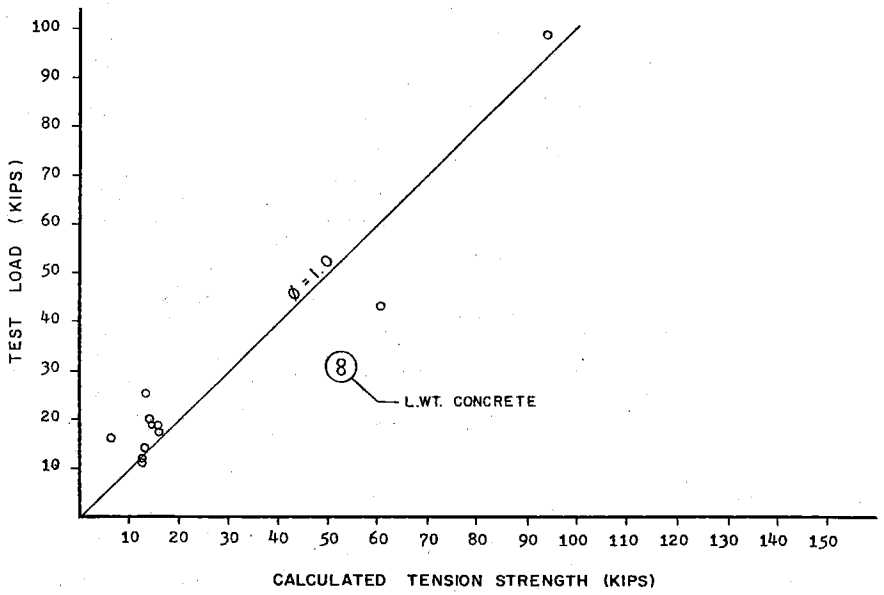

Fig. 7. Calculated tension strength [Eqs. (5) or (6)] versus test load.

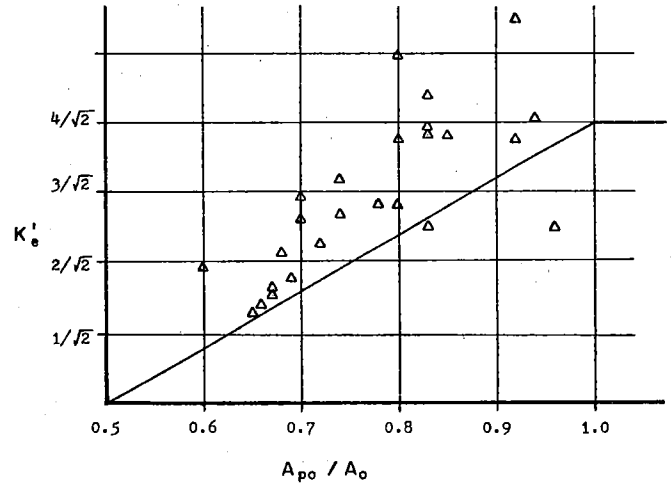

Fig. 8. Edge effect stress factor, K'_e versus partial to full cone surface area ratio, A_{po}/A_o.

correlations with edge effect test data. This is apparent in Figs. 3 and 5 (corresponding to Refs. 5 and 11), where more of the edge effect data points are scattered on the nonconservative side of the $\phi = 1.0$ line.

It should be noted that for Ref. 12 (Fig. 6), only six edge effect data points are available; the rest are eliminated due to the bursting criterion. Two of these six data points are on the nonconservative side.

Ref. 10 is a slight improvement over Refs. 5, 11, and 12 in that the multiplier used is the ratio of smaller full cone area to full cone area. This ratio is smaller than the ratio of partial cone area to full cone area and thus indirectly takes into account the second part in the edge effect. The correlation in Fig. 4 is better than in Figs. 3 and 5; however, it is still unsatisfactory. In the *PCI Design Handbook*,[2] the edge effect multiplier, d_e/l_e, is retained. This aspect will be discussed later.

To study the edge effect, since both parts of the edge vicinity (direct reduction of area of the cone and stress adjustment factor) are dependent on A_{po}/A_o, i.e., partial cone area to full cone area, $4/\sqrt{2}$ in Eq. (6) is replaced with K'_e. Then Eq. (6), for the edge effect included, may be written as:

$$P_{nc} = K'_e\ \sqrt{f'_c}A_o \qquad (8)$$

Based on a correlation with edge effect data points, K'_e can now be evaluated. By setting P(test)/P[calculated — Eq. (8)] = 1.0, K'_e can be evaluated and plotted versus A_{po}/A_o. This plot is shown in Fig. 8. The straight line correlation appears to be a reasonable lower bound and is given by:

$$K'_e = \frac{4}{\sqrt{2}}\left(2\frac{A_{po}}{A_o} - 1\right) \qquad (9)$$

and the pull-out strength with edge effect included is:

$$P_{nc} = \frac{4}{\sqrt{2}}\sqrt{f'_c}A_o\left(2\frac{A_{po}}{A_o} - 1\right) \qquad (10)$$

It should be noted that under the restriction that $A_{po}/A_o \leq 1.0$, Eq. (10) serves to calculate the pull-out strength with or

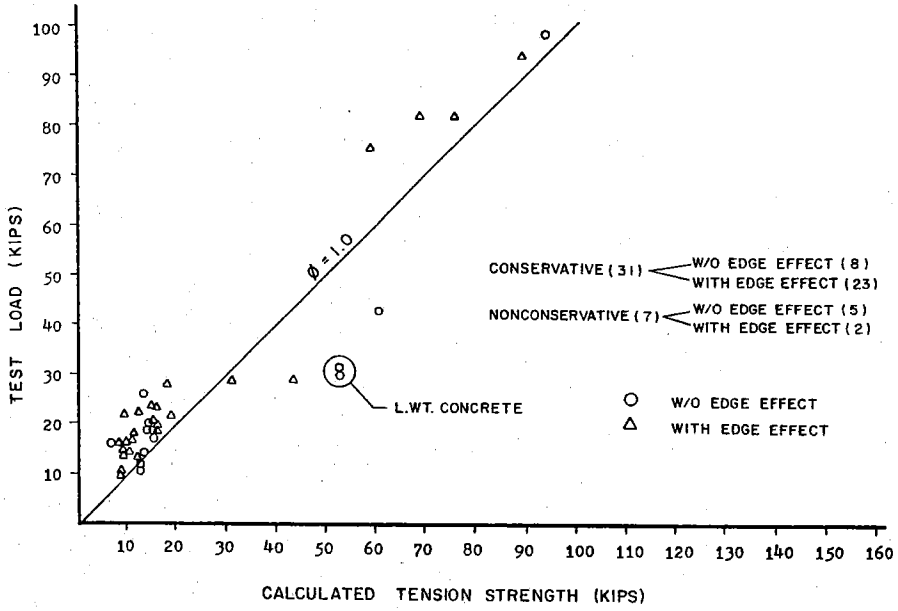

Fig. 9. Calculated tension strength [Eq. (10)] versus test load.

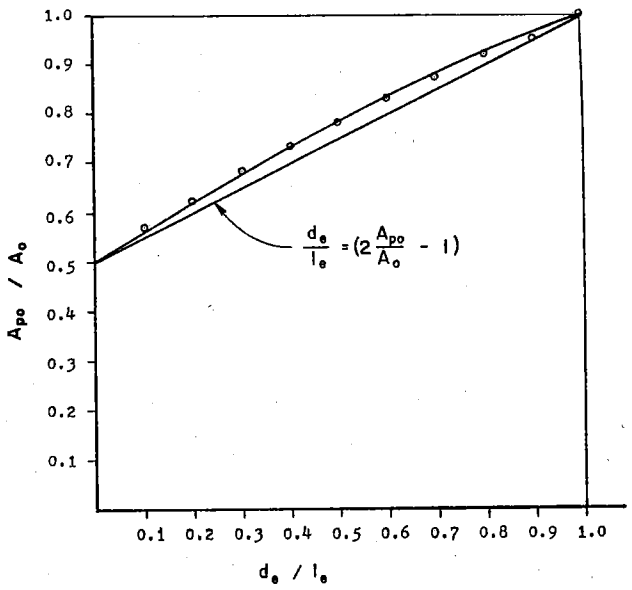

Fig. 10. Partial to full cone surface area ratio, A_{po}/A_o versus PCI² edge effect multiplier, d_e/l_e.

without the edge effect. Also, at the limit value of $A_{po}/A_o = 0.5$ (insert at edge), Eq. (10) results in $P_{nc} = 0$. The correlation of this equation with all data considered is shown in Fig. 9 and appears satisfactory.

The edge effect multiplier d_e/l_e first appeared in Ref. 9, and was based on test data from Ref. 14. Its plot versus A_{po}/A_o is shown in Fig. 10. The relationship is almost a straight line with the equation:

$$\frac{d_e}{l_e} = 2\frac{A_{po}}{A_o} - 1 \qquad (11)$$

It is interesting to note that this expression [Eq. (11)] is the same as that obtained from test data establishing K'_c in Eq. (8). The slight difference between the actual d_e/l_e values as shown in Fig. 10 and the straight line approximation should produce only a minor effect on correlation. Due to its simplicity, the Connection Details Committee has recommended continued use of d_e/l_e to account for the edge effect.

Replacing [2 (A_{po}/A_o) − 1] with (d_e/l_e) in Eq. (10) results in:

$$P_{nc} = \frac{4}{\sqrt{2}}\sqrt{f'_c}\,A_o\left(\frac{d_e}{l_e}\right) \qquad (12)$$

The correlation of Eq. (12) is shown in Fig. 11.

Tension Strength of a Stud Group

If the spacing between studs in a group is large, the strength of the group is calculated as the sum of individual stud tension strengths. However, if the spacing between studs is smaller than a certain critical value, individual failure cones cannot develop and thus the failure occurs along a composite surface. The *PCI Design Handbook*[2] suggests the use of a truncated pyramid (45 deg)

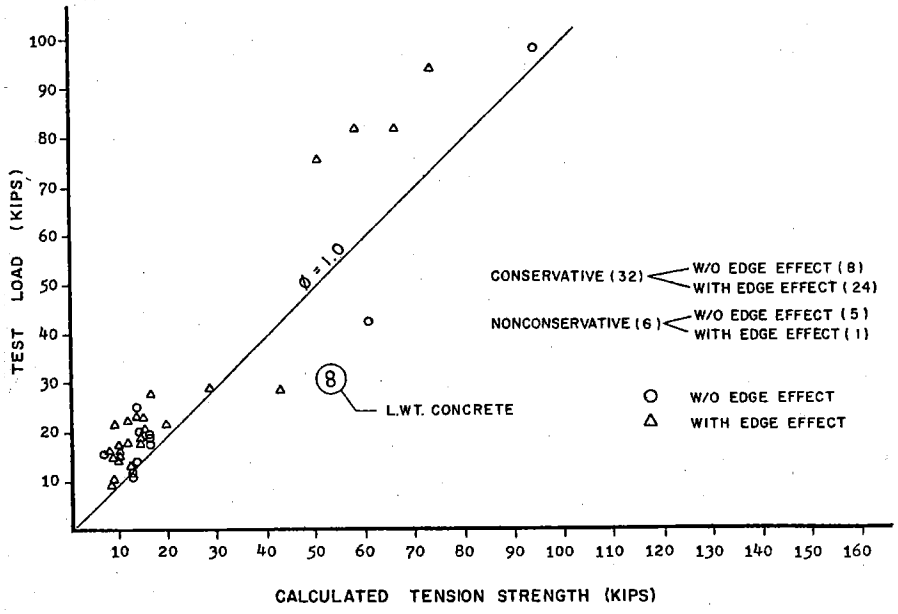

Fig. 11. Calculated tension strength [Eq. (12)] versus test load.

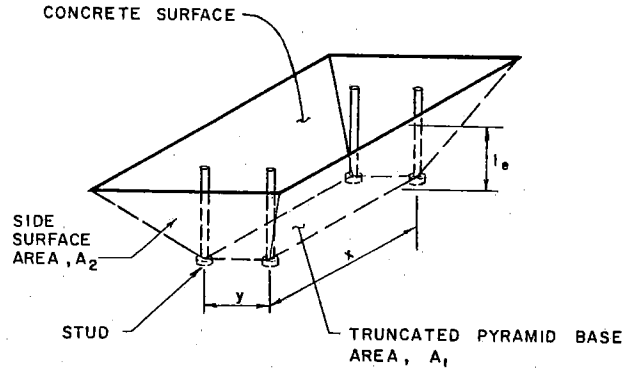

Fig. 12. Truncated pyramid failure for a stud group in tension.

failure surface as shown in Fig. 12.

The proposed revision to the shear cone strength indicates that the strength associated with the truncated pyramid failure must also be revised. This is done by taking a stress level of $4\sqrt{f'_c}$ on the base area (A_1 in Fig. 12) and $(4/\sqrt{2})\sqrt{f'_c}$ on the sloping sides (A_2 in Fig. 12). The resulting nominal strength equations are shown in Fig. 13 as P_{nc} values corresponding to thickness $h \geq (z+2l_e)/2$.

For stud groups in relatively thin members, it is likely that the failure surface would penetrate completely through the concrete causing a punching shear type failure as shown in Fig. 14. The tension strengths based on this mode of failure are also shown in Fig. 13 corresponding to thickness $h < (z+2l_e)/2$.

SHEAR STRENGTH

An excellent summary of the various procedures for calculating shear strength is given in Ref. 15. For the no edge effect condition, there are basically two methods. One is the empirical equation of Refs. 10 and 16 (same equation with different units used) and the other approach is based on shear-friction.[2,5,9]

Refs. 11, 12, and 17 assume that the concrete failure is precluded if the studs have sufficient development length and are located sufficiently away from free edges. Therefore, no calculation of direct shear strength based on concrete failure is given.

The likelihood of pull-out (cone type) failure of studs which are under shear loads is handled in the above procedures by either precluding such failures by using sufficient embedment as in Refs. 10, 11, 12, 14, and 17 or by specifying the tension strength as an upper bound on the direct shear strength as in Refs. 2, 5, and 9. The effect of vicinity to free edges in the direction of shear is taken into account in one of three ways:

(a) Multiplying the basic shear strength by a reduction factor (Refs. 10 and 14);
(b) A different empirical formula (Refs. 2, 5, and 9), and
(c) Modeling the failure surface as a semi-cone of a height equal to the edge distance (Refs. 11, 12, and 17).

While it is preferable to preclude concrete failures by providing sufficient embedment and sufficient edge distances, in many structures it is not feasible to do so. Consequently, considera-

Fig. 13. Stud groups in tension.

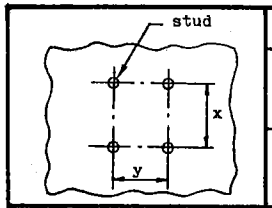	**Case 1: Not near a free edge***
	$h \geq (z^{\dagger}+2l_e)/2$ — $P_{nc} = 4\lambda\sqrt{f'_c}\,(x+2l_e)(y+2l_e)$
	$h < (z+2l_e)/2$ — $P_{nc} = 4\lambda\sqrt{f'_c}\,((x+2l_e)(y+2l_e) - A_R^{\ddagger})$
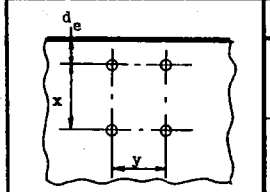	**Case 2: Free edge on one side**
	$h \geq (z+2l_e)/2$ — $P_{nc} = 4\lambda\sqrt{f'_c}\,(x+l_e+d_e)(y+2l_e)$
	$h < (z+2l_e)/2$ — $P_{nc} = 4\lambda\sqrt{f'_c}\,((x+l_e+d_e)(y+2l_e) - A_R)$
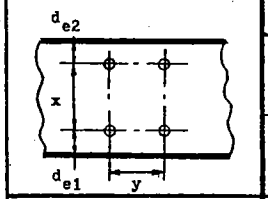	**Case 3: Free edges on 2 opposite sides**
	$h \geq (z+2l_e)/2$ — $P_{nc} = 4\lambda\sqrt{f'_c}\,(x+d_{e1}+d_{e2})(y+2l_e)$
	$h < (z+2l_e)/2$ — $P_{nc} = 4\lambda\sqrt{f'_c}\,((x+d_{e1}+d_{e2})(y+2l_e) - A_R)$
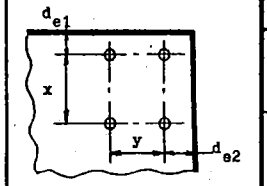	**Case 4: Free edges on 2 adjacent sides**
	$h \geq (z+2l_e)/2$ — $P_{nc} = 4\lambda\sqrt{f'_c}\,(x+l_e+d_{e1})(y+l_e+d_{e2})$
	$h < (z+2l_e)/2$ — $P_{nc} = 4\lambda\sqrt{f'_c}\,((x+l_e+d_{e1})(y+l_e+d_{e2}) - A_R)$
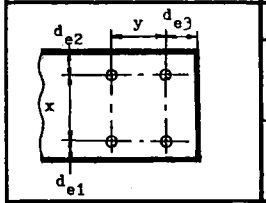	**Case 5: Free edges on 3 sides**
	$h \geq (z+2l_e)/2$ — $P_{nc} = 4\lambda\sqrt{f'_c}\,(x+d_{e1}+d_{e2})(y+l_e+d_{e3})$
	$h < (z+2l_e)/2$ — $P_{nc} = 4\lambda\sqrt{f'_c}\,((x+d_{e1}+d_{e2})(y+l_e+d_{e3}) - A_R)$
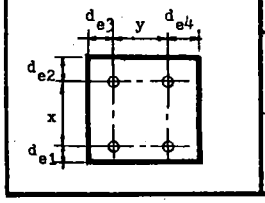	**Case 6: Free edges on 4 sides**
	$h \geq (z+2l_e)/2$ — $P_{nc} = 4\lambda\sqrt{f'_c}\,(x+d_{e1}+d_{e2})(y+d_{e3}+d_{e4})$
	$h < (z+2l_e)/2$ — $P_{nc} = 4\lambda\sqrt{f'_c}\,((x+d_{e1}+d_{e2})(y+d_{e3}+d_{e4}) - A_R)$

*Near a free edge implies $d_e < l_e$.

†"z" is equal to the lesser of the "x" and "y" values.

‡$A_r = (x + 2l_e - 2h)(y + 2l_e - 2h)$.

Note: The nominal tension strength (P_{nc}) values given in the table are obtained by using stress levels of $(4/\sqrt{2})\sqrt{f'_c}$ on the sloping sides area and $4\sqrt{f'_c}$ on the base area of the failure surface, respectively.

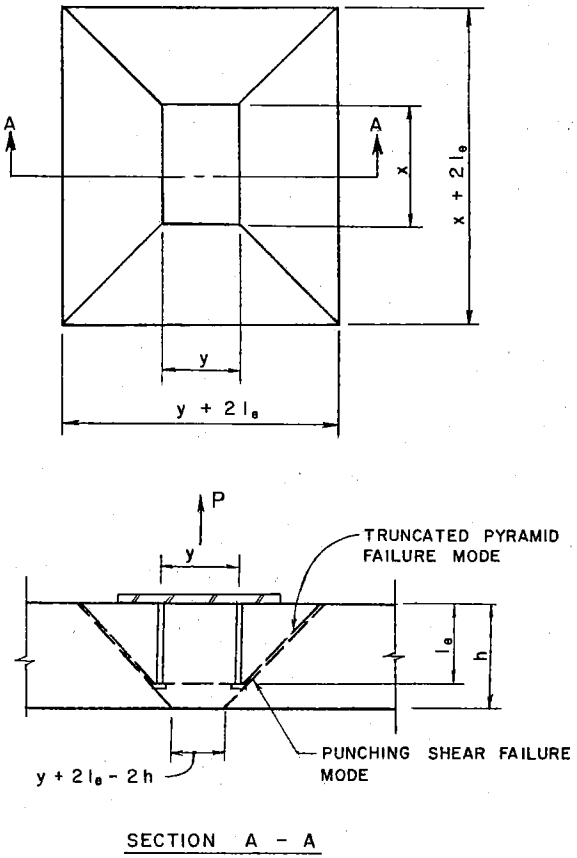

Fig. 14. Truncated pyramid and punching shear failures.

tion of limited embedment as well as short edge distance is included in this paper.

Shear Strength of Stud Located Away From Concrete Member Edge

Considering first the shear-friction model, the shear strength is given[2,5,9] as:

$$\phi V_c = \phi\, \mu A_b f_y$$

which for $\mu = 1.0$ (a conservative value according to Ref. 2), $\phi = 0.85$ and $f_y = 0.9 f_s$ is: $\phi V_c = 0.765 A_b f_s$.

In comparing this with the strength based on steel failure (Ref. 2), that is: $\phi V_s = 0.75 A_b f_s$, it is apparent that the shear-friction will never govern the shear strength. Also, the shear-friction model poses some conceptual difficulties. It appears that while a sufficiency of shear-friction strength would enable the connection to behave as a friction type connection, a deficiency would transform it into a bearing type connection.

Although the shear-load slip behavior would be different, the strength would eventually be dictated by either concrete failure due to thrusting of the stud against it or the stud steel failure. Therefore, unless additional testing and analyses are done to define various parameters, such as interface area, crack directions, etc., use of the shear-friction model is questionable.

Eq. (13) is an empirical equation from Ref. 16. Its correlation with test data is quite good,[14,16] even though it is not a lower bound correlation.

The following shows that this empirical formula [Eq. (13)] can be transformed easily into a much simpler equation with only a slight approximation:

$$V_{nc} = 1.106 A_s (f'_c)^{0.3} (E_c)^{0.44} \qquad (13)$$

where V_{nc} is expressed in kips, and f'_c and E_c are in ksi units. Converting these to psi units:

$$V_{nc} = 1.106 A_s \frac{(f'_c)^{0.3}}{(1000)^{0.3}} \frac{(E_c)^{0.44}}{(1000)^{0.44}}$$

$$V_{nc} = 6.66\,(10^{-3}) A_s (f'_c)^{0.3} (E_c)^{0.44} \qquad (13a)$$

which is the equation given in Ref. 10.

Substituting the ACI Code[13] concrete modulus $E_c = 33\, w^{1.5}\, (f'_c)^{0.5}$ in Eq. (13a) yields:

$$V_{nc} = 6.66\,(10^{-3}) A_s (f'_c)^{0.3} [33\, w^{1.5} (f'_c)^{0.5}]^{0.44}$$
$$= 31.02\,(10^{-3}) A_s (f'_c)^{0.52} w^{0.66} \qquad (13b)$$

Unit weight ratios and λ factors for various types of concrete are given in Table 1. It can be seen from Table 1 that for different weight concretes, only a slight approximation is needed to substitute $w^{0.66}$ in Eq. (13b) with.

Table 1. Unit weight ratios and λ factors for various types of concrete.

Type of concrete	w	$w^{0.66}$	$\frac{w^{0.66}}{w^{0.66*}}$	λ
Normal weight	145	26.7	1.0	1.0
Sand lightweight	120	23.6	0.87	0.85
All lightweight	90	19.5	0.73	0.75

*Normal weight concrete.

$$\lambda\, (w^{0.66})_{\text{N.wt.conc}} = \lambda\, (145)^{0.66} = \lambda\, (26.7)$$

Therefore,

$$V_{nc}\,(\text{kips}) = 828\,(10^{-3}) A_s \lambda\, (f'_c)^{0.52} \qquad (13c)$$

or

$$V_{nc}\,(\text{lbs}) = 828 A_s \lambda\, (f'_c)^{0.52} \qquad (13d)$$

Noting that $[(f'_c)^{0.52}/(f'_c)^{0.50}]$ for f'_c = 3000 to 7000 psi varies from about 1.17 to 1.19, it would cause only a minor approximation to use an average value of 1.18 and rewrite Eq. (13d) as:

$$*V_{nc} = 977 A_s \lambda \sqrt{f'_c} \qquad (14)$$

where V_{nc} is in lb and f'_c is in psi units.

The correlation of Eq. (14) with experimental data of Ref. 16, which appears to be the only applicable data available to date, is shown in Fig. 15. As can be seen, the equation does not provide a lower bound. For a lower bound correlation, a coefficient smaller than 977 in Eq. (14) must be used. For example, replacing 977 with 800, such that:

$$V_{nc} = 800 A_s \lambda \sqrt{f'_c} \qquad (15)$$

*Based on a correlation with test data of Ref. 16, Martin and Korkosz[8] report arriving at a value of $V_c = 900 A_s \lambda \sqrt{f'_c}$.

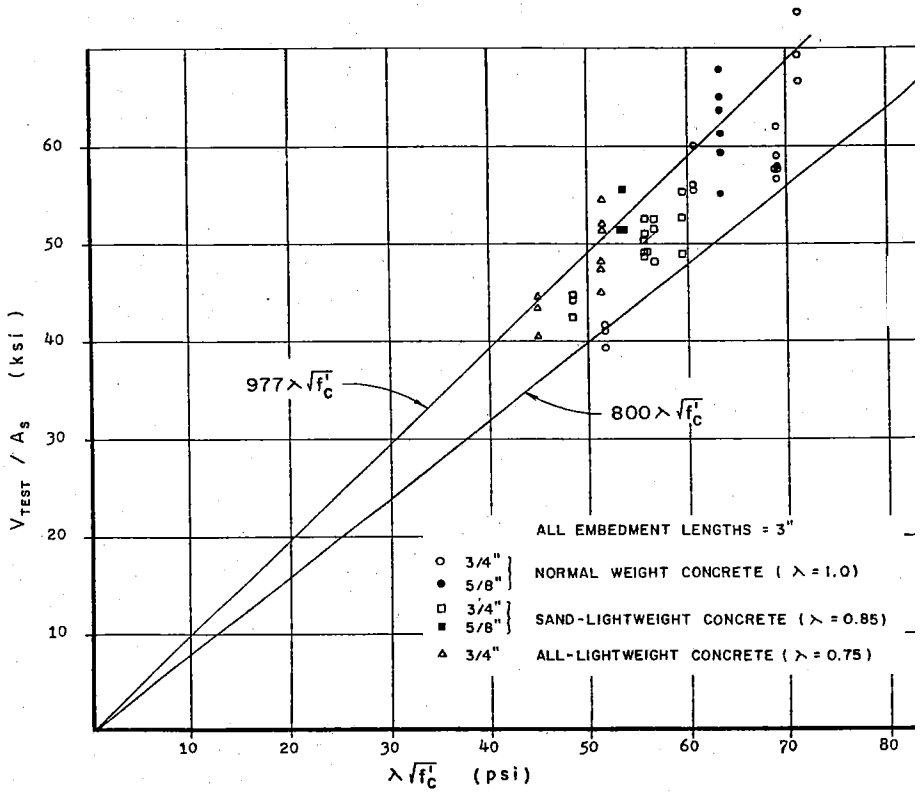

Fig. 15. Shear strength of studs (experimental data from Ref. 16).

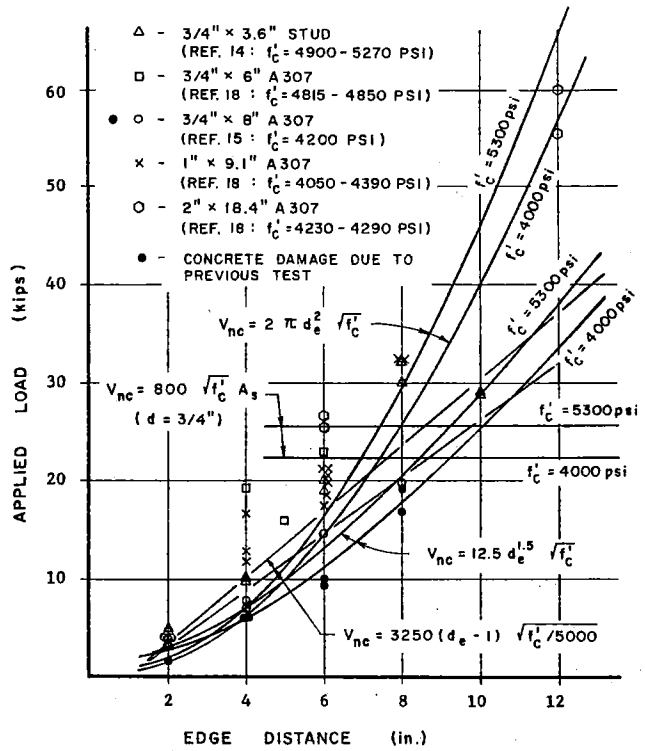

Fig. 16. Shear on studs located close to edge.

produces a lower bound correlation as shown in Fig. 15.

Consideration of the Edge Effect

When a stud is loaded in shear toward a free edge and if the edge distance is less than a certain critical value, the mode of failure typically is due to cracking of concrete in roughly a semi-conical shape.

As noted previously, Ref. 2 takes into account the edge effect by an empirical equation:

$$V_{nc} = 3250\,(d_e - 1)\,\frac{\sqrt{f'_c}}{\sqrt{5000}}$$

in which, factor ϕ is left out for the purpose of correlation with test data. Fig. 16 shows this correlation with experimental data found in Refs. 14, 15, and 18 (it appears that this is all the data available for short edge distance without confining reinforcement).

Even disregarding the data points related to tests where there was previous damage (solid circles in Fig. 16), the correlation of the above equation does not appear to be satisfactory. The modification factor for the edge effect of Refs. 10 and 14 is also a straight line and is even more nonconservative than the PCI equation, and thus, it is not shown.

Refs. 11 and 12 assume a semi-cone failure surface with the height equal to the edge distance and a "normal to the surface" stress level of $4\sqrt{f'_c}$. (This stress level is the same as that used in the tension strength concrete failure model.) For a 45 deg cone, $4\sqrt{f'_c}$ results in $(4/\sqrt{2})\sqrt{f'_c}$ for both shear and tension resistance. Thus:

$$V_{nc} = 2\,\pi\,d_e^2\,\sqrt{f'_c} \qquad (16)$$

A plot of this equation for $f'_c = 4000$ psi and $f'_c = 5300$ psi (range of f'_c values for available test data) is also shown in Fig. 16. Again, ignoring the solid circles and observing the cutoff provided by Eq. (15) [no edge effect], the correlation of Eq. (16) appears satisfactory.

A closer examination of the data in Fig. 16 suggests that a better fit might be obtained by considering an equation in which the power of d_e is some value between 1 and 2. The equation:

$$V_{nc} = 12.5\,(d_e)^{1.5}\,\sqrt{f'_c} \qquad (17)$$

was considered and its correlation is also shown in Fig. 16. However, due to the rationality of the ACI 349[12] model, and also the desirability of consistency between different procedures, Eq. (16) is included in the design procedure.

The limiting value of the edge distance, d_e, which dictates use of either Eq. (15) or Eq. (16) is obtained by equating the two. Thus:

$$2\pi d_e^2 \lambda \sqrt{f_c'} = 800 A_s \lambda \sqrt{f_c'}$$

$$\text{or, } 2\pi d_e^2 \lambda \sqrt{f_c'} = 800 \left(\frac{\pi}{4} d^2\right) \lambda \sqrt{f_c'}$$

$$\text{or, } d_e = 10\,d \qquad (18)$$

Consequently if $d_e > 10\,d$, shear strength is governed by Eq. (15); if $d_e < 10\,d$, the shear strength is governed by Eq. (16).

As noted earlier, Refs. 2, 5, and 9 specify the tension strength as an upper bound on the direct shear strength to preclude pull-out failure of studs under shear loads. Apparently, the similarity between the failure surface observed in some shear tests and the pull-out failure surface, namely, the cone type, was taken as a justification for this provision. However, examination of shear test data does not support this practice.

The comprehensive compilation of shear test data reported in Ref. 18 is reanalyzed with and without the pull-out strength, P_{nc} limitation and plotted in Fig. 17. The plot in Fig. 17 is in terms of Test No. (as noted in Ref. 18) versus ratio of observed shear strength, V_c (test), to calculated [using Eqs. (15) and (16)] shear strength, V_{nc} (calculated).

Of the 103 tests, 92 relate to concrete failure and are shown in Fig. 17. The remaining 11 relate to steel failure condition. It is noted that these data cover a wide range of parameters related to embedment length, stud/anchor diameter, and concrete density.

In Fig. 17, a data point falling on V_c (test)/V_{nc} (calculated) line of 1.0 indicates a perfect correlation while those falling above and below this line indicate conservative and nonconservative correlations, respectively. As seen in Fig. 17, the correlation of these data without the pull-out strength, P_{nc} limitation is remarkably good, particularly if the seven data points where prior cracking or damage was documented are excluded.

The correlation with the pull-out strength limitation is unnecessarily conservative. Furthermore, it does not affect the few data points falling below the perfect correlation line. Therefore, the authors find little merit in using the pull-out strength as an upper bound on shear strength and recommend its elimination.

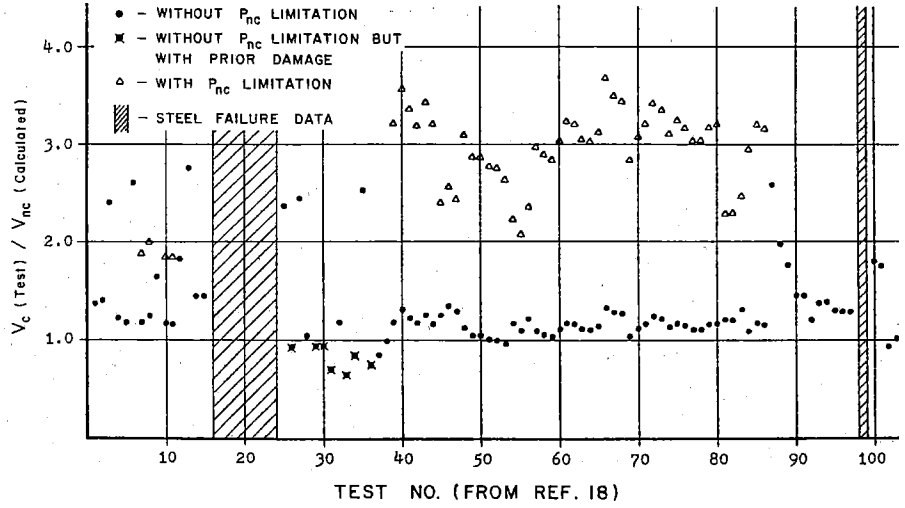

Fig. 17. Effect of pull-out strength limitation on shear strength.

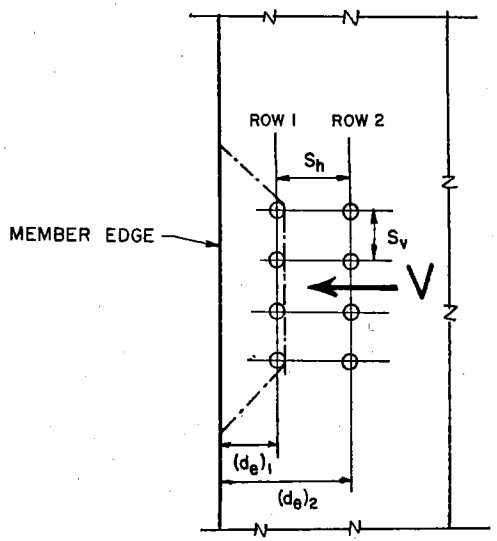

Fig. 18. Stud group under shear.

Shear Strength of Stud Groups

There appears to be no test data to rely on for the development of design equations for this example. The following observations were used by the Connection Details Committee as guidelines for recommendations included in the design procedure. Examining a connection with two rows of connectors, Rows 1 and 2 in Fig. 18, the following observations can be made:

1. If the strength of the studs in the leading row (Row 1) is not affected by the edge distance [i.e., Eq. (15) governs], then it appears reasonable to take the total shear strength equal to n times the "per stud shear strength" as obtained from Eq. (15) provided the spacing S_h is not too small. If the spacing S_h is small, the strength of the group could be taken as the strength of one row.

2. If the strength of the studs in Row 1 is governed by Eq. (16) (i.e., edge distance is small), then failure of the concrete plug between this row and the free edge is likely to make the back row vulnerable unless the spacing S_h is large. [Note: The critical edge distance which bifurcates calculation of strength between Eqs. (15) and (16) is equal to 10 times the stud shank diameter.] It appears reasonable that the strength of the back row be calculated with the limitation $(d_e)_2 = S_h$. The strength of the group then should be limited to either the strength of Row 1 when $S_h \leq (d_e)_1$, or the strength of Row 2 when $S_h > (d_e)_1$.

3. In determining the strength of Row 1 under the edge effect condition, due account must be taken of the spacing between studs, S_v, in Fig. 18. If S_v is large, non-overlapping semi-cones would develop. Thus, the strength of Row 1 may be taken equal to n_1 times the per stud strength as given by Eq. (16), where n_1 is the number of studs in Row

1. If the spacing S_v is small, the failure may be along a composite 45 deg plug (along dash-dot line in Fig. 18) — similar to the truncated cone for the stud group in tension. In that case the strength should be limited to the area of the plug times a stress of $4/\sqrt{2}$ (or $2.8)\sqrt{f'_c}$.

COMBINED TENSION AND SHEAR STRENGTH

For designing studs under combined tension and shear loads, the following type of interaction equation has been generally used:

$$\left(\frac{P_u}{\phi P_{nc}}\right)^K + \left(\frac{V_u}{\phi V_{nc}}\right)^K \leq 1.0 \quad (19)$$

where P_u and V_u are the applied factored tension and shear loads, respectively, P_{nc} and V_{nc} are the nominal direct tension and direct shear strengths, respectively.

Ref. 14 indicates a value of 5/3 for the exponent K, while Ref. 2 uses 4/3.

The test data of Ref. 14 (apparently the only data available for combined loads) is replotted in Fig. 19 with a slight modification: the stress coordinate in Ref. 14 is replaced with a load coordinate for convenience. Also, four data points of Ref. 14 are excluded from Fig. 19. Three of the excluded data points pertain to lightweight concrete and, in view of the poor correlation of lightweight concrete in tension only situations (see Figs. 2 through 7, 9, and 11), it seems meaningless to carry out correlation under combined loads.

The fourth excluded data point pertains to normal weight concrete; however, it is the only data point with a different embedment length and cannot be included in Fig. 19. Thus, all the data in Fig. 19 are for ¾ x 4 in. studs in normal weight concrete and there is no edge effect.

Calculating the nominal strength P_{nc} and V_{nc} by Eqs. (7) and (15), respectively:

$$P_{nc} = 2.8\,\lambda\,\sqrt{f'_c}\,[\sqrt{2}\,\pi\,l_e\,(l_e + d_h)] \quad (7)$$
$$= 2.8\,(1.0)\,\sqrt{5000}\,[\sqrt{2}\,\pi\,(3.625)\,(3.625 + 1.25)]/1000$$
$$= 15.7 \text{ kips}$$

$$V_{nc} = 800\,\lambda\,\sqrt{f'_c}\,A_b \quad (15)$$
$$= 800\,(1.0)\,\sqrt{5000}\,(0.44/1000)$$
$$= 24.9 \text{ kips}$$

and substituting in Eq. (20) with $\phi = 1.0$ results in:

$$\left(\frac{P_u}{15.7}\right)^K + \left(\frac{V_u}{24.9}\right)^K \leq 1.0 \quad (20)$$

Plots of Eq. (20) with $K = 4/3$, $K = 5/3$, and also $K = 2$ are shown in Fig. 19. While $K = 4/3$ is unduly conservative, $K = 5/3$ may be acceptable. $K = 2$ also seems to provide a good fit and is still a reasonable lower bound. Also $K = 2$ is the same as in the interaction equation for steel failure.

One additional observation relates to the use of factor ϕ under the exponent in Eq. (19). In doing so, one is effectively using a lower strength reduction factor; for example, when $\phi = 0.85$, $\phi^2 = 0.72$. Since all nominal strength equations are based on lower bound correlations, it seems appropriate to take ϕ outside the exponent. Rewriting Eq. (19) with this change and $K = 2$:

$$\frac{1}{\phi}\left[\left(\frac{P_u}{P_{nc}}\right)^2 + \left(\frac{V_u}{V_{nc}}\right)^2\right] \leq 1.0 \quad (21)$$

Eq. (21) is included in the design procedure.

DESIGN PROCEDURE — IN-PLACE STRENGTH OF HEADED STUDS

Headed studs are often used to connect precast concrete members. In transferring forces between interconnected members, the headed studs may be subjected to direct tension, direct shear or a combination of the two. In designing headed studs, the in-place strength is taken as the lesser of the strengths based on concrete failure and steel failure.

The strength equations for concrete failure given below are established on the basis of lower bound correlation with available test data, and are applicable to studs which are previously welded to steel plates or members, and embedded in unconfined concrete. The equations are also applicable to inserts, headed bolts, and expansion anchors.

Confinement of the concrete, either from applied compressive loads or from reinforcement, is known to increase the capacity; however, due to limited research in this area, acceptable design equations which include these effects are not available.

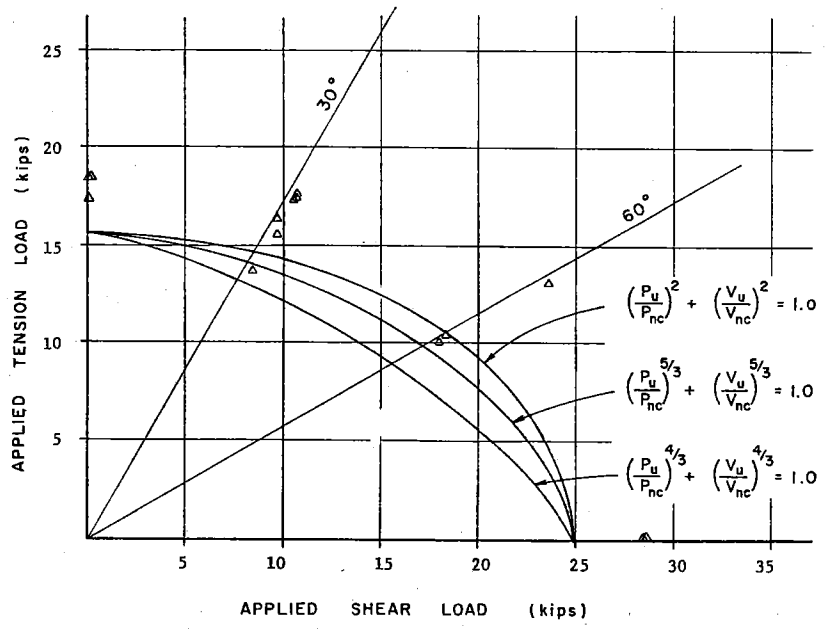

Fig. 19. Studs under combined shear and tension (experimental data from Ref. 14).

Tension

The design tension strength governed by concrete failure is:

$$\phi P_{nc} = \phi\,2.8\,\lambda\,\sqrt{f'_c}\,A_o \quad (D1)$$

where

ϕ = 0.85

λ = 1.0 for normal weight concrete, 0.85 for sand lightweight concrete and 0.75 for all lightweight concrete

A_o = area of the assumed failure surface which, for a stud not located near a free edge, is taken to be that of a 45 deg cone.

Using the 45 deg cone area and ϕ = 0.85, Eq. (D1) may be written as:

$$\phi P_{nc} = 10.7\,\lambda\,\sqrt{f'_c}\,l_e\,(l_e + d_h) \quad (D1a)$$

For a stud located closer to a free edge than the embedment length l_e, the de-

sign tension strength given by Eq. (D1) or Eq. (D1a) should be reduced by multiplying it with C_{es}:

$$C_{es} = \frac{d_e}{l_e} \leq 1.0 \qquad \text{(D2)}$$

where d_e is the distance measured from the stud axis to the free edge.

If a stud is located in the corner of a concrete member, Eq. (D2) should be applied twice, once for each edge distance, d_e.

For a group of studs, if the spacing between studs is smaller than a certain critical value, the concrete failure surface may be along a truncated pyramid rather than separate shear cones. Therefore, for stud groups, the design tension strength should be taken as the lesser of the values based on the sum of the individual stud strengths and that associated with the truncated cone pyramid type failure (P_{nc}) values corresponding to $h \geq (z + 2l_e)/2$ (Fig. 13).

For stud groups in members whose thicknesses are small, it is likely that the failure surface would penetrate the thickness of the member as shown in Fig. 14, and the design tension strength should be limited accordingly. The strengths based on this type of failure are the (P_{nc}) values in Fig. 13 corresponding to $h < (z + 2l_e)/2$.

The design tension strength per stud as governed by steel failure is:

$$\phi P_{ns} = \phi f_{ut} A_b \qquad \text{(D3)}$$

where

A_b = cross-sectional areas of stud shank

f_{ut} = yield strength of steel in tension and may be taken equal to $0.9f_s$, where f_s is the ultimate tensile strength of steel.

ϕ = 1.0

Shear

The design shear strength governed by concrete failure is dependent on the edge distance, d_e and is given by the following equations:

$$\phi V_{nc} = \phi\, 800\, \lambda\, \sqrt{f'_c}\, A_b, \text{ if } d_e \geq 10d \qquad \text{(D4)}$$

$$\phi V_{nc} = \phi\, \lambda\, \sqrt{f'_c}\, 2\pi d_e^2, \text{ if } d_e < 10d \qquad \text{(D5)}$$

where ϕ = 0.85 and d is the nominal diameter of stud shank.

For groups of studs, the design shear strength should be taken as the smallest of:

(1) The strength of the weakest stud [based on Eqs. (D4) and (D5)] times the number of studs,

(2) The strength of the row of studs nearest the free edge in the direction of shear times the number of rows, and

(3) The strength of the row farthest from the free edge in the direction of shear.

The design shear strength per stud as governed by steel failure is:

$$\phi V_{ns} = \phi\, f_{vv} A_b \qquad \text{(D6)}$$

where f_{vv} is the yield strength of steel in shear and may be taken equal to 0.75 f_s, and ϕ = 1.0.

Combined Tension and Shear

Design strength of studs under combined tension and shear should satisfy the following interaction equations:

Concrete failure:

$$\frac{1}{\phi}\left[\left(\frac{P_u}{P_{nc}}\right)^2 + \left(\frac{V_u}{V_{nc}}\right)^2\right] \leq 1.0 \qquad \text{(D7)}$$

where ϕ = 0.85, and P_u and V_u are the factored tension and shear loads, respectively.

Steel failure:

$$\frac{1}{\phi}\left[\left(\frac{P_u}{P_{ns}}\right)^2 + \left(\frac{V_u}{V_{ns}}\right)^2\right] \leq 1.0 \qquad \text{(D8)}$$

where ϕ = 1.0.

NUMERICAL EXAMPLES

The following two numerical examples illustrate the design procedure described in the previous section.

EXAMPLE 1

Determine if studs are adequate for the connection shown in Fig. 20. The loads on the bracket include appropriate load factors. Assume that f'_c = 5000 psi and that normal weight concrete is used.

Strength Based on Concrete

(A) Tension (group of top six studs):

1. Strength based on individual cones with edge effect.

d_e = 5 in., l_e = 6 in., d = ⅝ in., d_h = 1.25 in.

Using Eqs. (D1a) and (D2):

$$\phi P_{nc} = 10.7\, \lambda\, \sqrt{f'_c}\, l_e\, (l_e + d_h)\, (C_{es})$$
$$= 10.7\, (1.0)\, (\sqrt{5000})\, (6)\, (6 + 1.25)\, (5/6)/1000$$
$$= 27.4 \text{ kips}$$

ϕP_{nc} (group) = 6 (27.4) = 164.4 kips

or P_{nc} = 164.4/0.85 = 193.4 kips

2. Strength based on truncated pyramid failure (Fig. 13, Case 3).

$$P_{nc} = 4\, \lambda\, \sqrt{f'_c}\, (x + d_{e1} + d_{e2})\, (y + 2l_e)$$
$$= 4\, (1.0)\, (\sqrt{5000})\, (6 + 5 + 5)\, [3 + 2\, (6)]$$
$$= 67.9 \text{ kips (controls)} < 193.4 \text{ kips}$$

3. Required tension strength, P_u, for group of top studs.

Direct tension, N_u = 12 kips

Tension, T_u, resulting from moment:

M_u = 75(6) = 450 kip-in.

$T_u\, (j_u d) = T_u\, [d - (a/2)] = 450$

$$T_u \left[d - \frac{T_u}{0.85 f'_c\, b\, (2)} \right] = 450$$

$$T_u \left[11.0 - \frac{T_u}{0.85\, (5)\, (10)\, (2)} \right] = 450$$

T_u = 42.9 kips

$P_u = T_u + N_u$ = 42.9 + 12 = 54.9 kips

(B) Shear (12 studs)

1. Nominal shear strength (⅝ in. stud, $d_e > 10d$). Using Eq. (D4):

$$\phi V_{nc} = \phi\, (800)\, \lambda\, \sqrt{f'_c}\, A_b$$
$$= \phi\, (800)\, (1.0)\, (\sqrt{5000})\, [(\pi/4)\, (⅝)^2]$$
$$= \phi\, (17.4)$$

V_{nc} (group) = 12 (17.4) = 209 kips

2. Required shear strength:

V_u = 75 kips

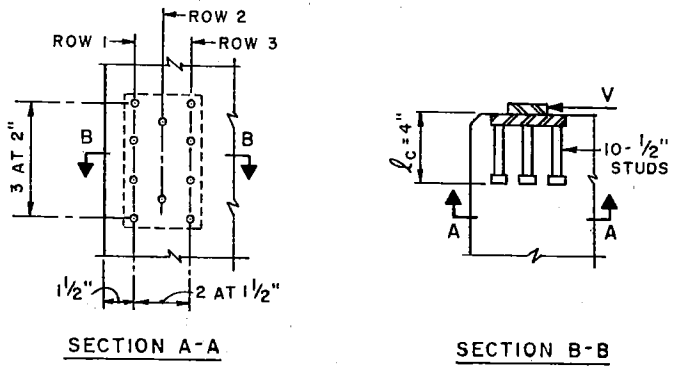

Fig. 20. Cross section of stud connection for Example 1.

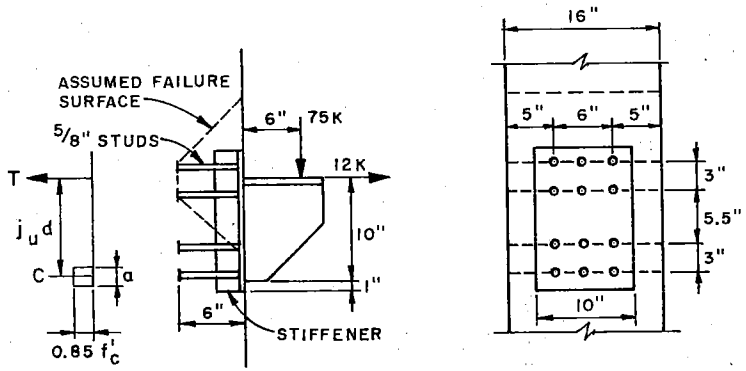

Fig. 21. Cross section of stud group for Example 2.

(C) Combined loads—Using Eq. (D7):

$$\frac{1}{\phi}\left[\left(\frac{P_u}{P_{nc}}\right)^2+\left(\frac{V_u}{V_{nc}}\right)^2\right]\leq 1.0$$

$$\frac{1}{0.85}\left[\left(\frac{54.9}{67.9}\right)^2+\left(\frac{75}{209}\right)^2\right]$$

$$= 0.92 < 1.0 \text{ (ok)}$$

Strength Based on Steel

(A) Tension (group of top six studs)
Using Eq. (D3):

$$\phi P_{ns} = P_{ns} = f_{ut} A_b$$
$$= (0.9)\ (60)\ (\pi/4)\ (5/8)^2$$
$$= 16.6 \text{ kips}$$
$$P_{ns} \text{ (group)} = 6\ (16.6) = 99.6 \text{ kips}$$

(B) Shear (12 studs)—Using Eq. (D6):

$$\phi V_{ns} = V_{ns} = f_{yv} A_b$$
$$= (0.75)\ (60)\ (\pi/4)\ (5/8)^2$$
$$= 13.8 \text{ kips}$$
$$V_{ns} \text{ (group)} = 12\ (13.8) = 165.6 \text{ kips}$$

(C) Combined loads—Using Eq. (D8):

$$\frac{1}{\phi}\left[\left(\frac{P_u}{P_{ns}}\right)^2+\left(\frac{V_u}{V_{ns}}\right)^2\right]\leq 1.0$$

$$\frac{1}{1.0}\left[\left(\frac{54.9}{99.6}\right)^2+\left(\frac{75}{165.6}\right)^2\right]$$

$$= 0.51 < 1.0 \text{ (ok)}$$

Thus, the connection is adequate.

EXAMPLE 2

Calculate the design shear strength of the stud group in a column. Assume that f'_c = 5000 psi and that normal weight concrete is used. The sections to be analyzed are shown in Fig. 21.

Strength Based on Concrete

(A) For studs in Row 1, d_e = 1.5 in. < 10 d (= 5 in.). Using Eq. (D5):

$$\phi V_{nc} = \phi\ \lambda\ \sqrt{f'_c}\ 2\ \pi\ d_e^2$$
$$= 0.85\ (1.0)\ (\sqrt{5000})\ (2\pi)\ (d_e)^2$$
$$= 377.6\ (d_e)^2$$
$$= 377.6\ (1.5)^2$$
$$= 850 \text{ lb per stud}$$

(B) For studs in Row 2, d_e = 3 in. < 10 d.

$$\phi V_{nc} = 377.6\ (3)^2 = 3398 \text{ lb per stud}$$

(C) For studs in Row 3, d_e = 4.5 in. < 10 d.

$$\phi V_{nc} = 377.6\ (4.5)^2 = 7646 \text{ lb per stud}$$

The design shear strength of the group is the smallest of:

1. 10 (850) = 8500 lb (controls)
2. 4 (850) (3) = 10,200 lb
   or 2 (3398) (3) = 20,388 lb
3. 4 (7646) = 30,584 lb

Strength Based on Steel

Using Eq. (D6):

$$\phi V_{ns} = \phi\ f_{yv} A_b$$
$$= 1.0\ (0.75)\ (60{,}000)\ (\pi/4)\ (1/2)^2$$
$$= 9000 \text{ lb per stud}$$
$$\phi V_{ns} \text{ (group)} = 10\ (9000) = 90{,}000 \text{ lb} > \phi V_{nc}$$

Thus, the design shear strength of the group is 8500 lb and is governed by the concrete strength.

CLOSING REMARKS

The design procedure included in this paper updates the current *PCI Design Handbook* procedure by taking into account the latest reported information and experience shared by many with the authors. An important consideration in the development of the proposed design equations has been a careful re-examination of previously reported test data and analyses.

With respect to test data on this subject, it is apparent that such data is scarce. It is hoped that this paper will enhance interest in additional experimental and analytical research by manufacturers of inserts, as well as by others.

ACKNOWLEDGMENT

The authors sincerely acknowledge the contributions of the members of the Connection Details Committee of the Prestressed Concrete Institute who shared their experiences and provided reviews of an earlier draft of the paper. The authors also wish to thank Peter Courtois, Les Martin, and Ray McCann for their valuable input.

* * *

Discussion of this paper is invited. Please send your comments to PCI Headquarters by November 1, 1985

REFERENCES

1. Klingner, R. E., and Mendonca, J. A., "Tensile Capacity of Short Anchor Bolts and Welded Studs," *ACI Journal*, Proceedings V. 79, No. 1, July-August 1982.
2. *PCI Design Handbook – Precast and Prestressed Concrete*, 2nd Edition, Prestressed Concrete Institute, Chicago, Illinois, 1978.
3. *PCI Manual on Design of Connections for Precast, Prestressed Concrete*, Prestressed Concrete Institute, Chicago, Illinois, 1973.
4. Shaikh, A. F., "In-Place Tension and Shear Strength of U-Type Anchor Bolts," ACI Committee 355 Symposium — Anchorage to Concrete, Los Angeles, California, March 1983.
5. *PCI Manual for Structural Design of Architectural Precast Concrete*, Prestressed Concrete Institute, Chicago, Illinois, 1977.
6. Raths, C. H., "Production and Design of Architectural Precast Concrete," PCI JOURNAL, V. 12, No. 3, June 1967, pp. 18-43.
7. "Precast-Prestress Concrete Handbook," Dayton Superior Corporation, Miamisburg, Ohio, 1983.
8. Martin, L. D., and Korkosz, W. J., "Connections for Precast Prestressed Concrete Buildings, Including Earthquake Resistance," Technical Report No. 2, Prestressed Concrete Institute, Chicago, Illinois, March 1982.
9. "KSM Structural Engineering Aspects of Headed Anchors and Deformed Bar Anchors in the Concrete Construction Industry," KSM Fastening Systems Division, Omark Industries, Moorestown, New Jersey, 1974.
10. "Embedment Properties of Headed Studs," *Design Data* 10, TRW Nelson Division, Lorain, Ohio, 1974.
11. "Concrete Anchorages," *TVA Civil Design Standard*, No. DS-C6.1, Tennessee Valley Authority, Knoxville, 1975.
12. ACI Committee 349, "Proposed Addition to: Code Requirements for Nuclear Safety Related Concrete Structures (ACI 349 — 76)," *ACI Journal*, Proceedings V. 75, No. 8, August 1978.
13. ACI Committee 318, "Building Code Requirements for Reinforced Concrete (ACI 318-83)," American Concrete Institute, Detroit, Michigan, 1983.
14. McMackin, P. J., Slutter, R. G., and Fisher, J. W., "Headed Steel Anchors Under Combined Loading," *AISC Engineering Journal*, 2nd Quarter, April 1973.
15. Klingner, R. E., Mendonca, J. A., and Malik, J. B., "Effect of Reinforcing Details on Shear Resistance of Anchor Bolts Under Reversed Cyclic Loading," *ACI Journal*, Proceedings V. 79, No. 1, January-February 1982.
16. Ollgaard, J. G., Slutter, R. G., and Fisher, J. W., "Shear Strength of Stud Connectors in Lightweight and Normal Weight Concrete," *AISC Engineering Journal*, V. 8, No. 2, April 1971.
17. Cannon, R. W., Burdette, E. G., and Funk, R. R., "Anchorage to Concrete," Tennessee Valley Authority, Knoxville, December 1975.
18. Klingner, R. E., and Mendonca, J. A., "Shear Capacity of Short Anchor Bolts and Welded Studs," *ACI Journal*, Proceedings V. 79, No. 5, September-October 1982.

* * *

APPENDIX — NOTATION

A_o = surface area of full cone
A_{pc} = projected circle area
A_{cy} = concentric cylinder area
A_{po} = surface area of partial cone
A_b, A_s = nominal gross cross-sectional area of anchor shank
d = nominal diameter of anchor shank
d_e = edge distance (distance from center of anchor shank to the free edge)
d_h = nominal diameter of anchor head
E_c = modulus of elasticity of concrete
f'_c = specified 28-day compressive strength of concrete
f_s, f_{ut} = ultimate tensile strength of steel
f_y, f_{yt} = yield strength of steel in tension
f_{yv} = yield strength of steel in shear
l_e = embedment length (distance from surface of concrete to start of anchor head)
P_{nc} = nominal tensile capacity of anchor as governed by concrete failure
P_{ns} = nominal tensile strength of anchor as governed by steel failure
P_u = applied factored tension load
V_{nc} = nominal shear strength of anchor as governed by concrete failure
V_{ns} = nominal shear strength of anchor as governed by steel failure
V_u = applied factored shear load
w = unit weight of concrete
α = angle of inclination of conical concrete failure surface
ϕ = strength reduction factor
λ = 1.0 for normal weight concrete, 0.85 for sand-lightweight concrete, 0.75 for all-lightweight concrete

* * *